Regular Article

ANALYTICAL AND BIOANALYTICAL CHEMISTRY RESEARCH

Published by the Iranian Chemical Society

Anal. Bioanal. Chem. Res., Vol. 9, No. 1, 101-111, January 2022.

Synthesize of Iron-Polyphenol Nanohydrogel from Melia Azedarach Fruit Extract and its Application as a Flocculant for Coagulation and Removal of Disperse Yellow 211

Mohammad Reza Parsaeian[a], Shayessteh Dadfarnia[a,*], Ali Mohammad Haji Shabani[a] and Reza Hafezi Moghaddam[a,b]

[a]*Department of Chemistry, Faculty of Science, Yazd University, Yazd, Iran*

[b]*Central Iran Research Complex, Nuclear Science and Technology Research Institute, Yazd, Iran*

(Received 19 May 2021 Accepted 7 September 2021)

Melia azedarach fruit extract is used to synthesize iron-polyphenol nanohydrogel and its capability as a flocculant in coagulation and removal of Disperse Yellow 211 dye from the aqueous solution is examined. The structure of iron-polyphenol nanohydrogel is studied by Fourier transform infrared spectroscopy, field emission scanning electron microscopy, X-ray diffraction, Brunauer-Emmett-Teller analysis, and zeta potential. The field emission scanning electron microscopy analysis indicates that in situ-cross-linking of polyphenols of Melia azedarach extract by ferric ions resulted in the formation of nanohydrogel containing particles in the range of 23-35 nm. Experiments confirmed that the prepared iron-polyphenol nanohydrogel has the excellent ability as the flocculant for coagulation and removal of the Disperse Yellow 211 dye in the pH range of 4.0-8.0, at room temperature. The required time for obtaining equilibrium at different concentrations of dye is ~ 50 min, and in this period, 200 mg l^{-1} of dye solution is 92% decolorized. The best-fitted model for experimental data is found to be the second-order kinetics and Langmuir thermodynamic indicating the sorption occurs in a monolayer and is governed by chemisorption. The maximum capacity of the sorbent is 1111.1 mg g^{-1}.

Keywords: Green synthesis, Iron-polyphenol complex, Nanohydrogel, Adsorptive flocculation, Melia azedarach fruit, Disperse Yellow 211 dye

INTRODUCTION

Water is a valuable vital substance and access to clean water is essential for the survival of humans, living organisms on the earth, and water needy industrials. With the rapid growth of the population and the development of industries, the protection of water resources is a public duty, and recycling municipal, industrial and agricultural effluents are very important [1]. Discharge of effluents into water bodies can cause a gradual accumulation of pollutants in living organisms [2]. The entry of effluents containing organic dyes into the water sources affects the water quality parameters such as pH, dissolved oxygen, turbidity, chemical oxygen demand (COD), and light penetration [3]. For example, the presence of disperse dyes such as Yellow 211 (Fig. 1), a mono azo dye, extensively used in the paper

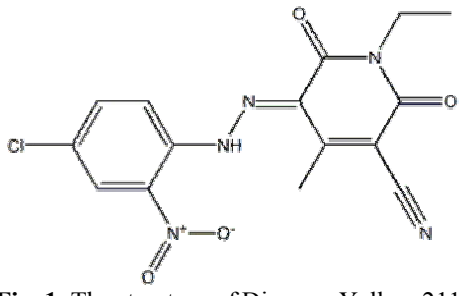

Fig. 1. The structure of Disperse Yellow 211.

Corresponding author. E-mail: sdadfarnia@yazd.ac.ir

and textile industry, in the effluent causes reflection or scattering of the sunlight in the water bodies [4]. Thus, it prevents the penetration of the light into the lower levels of water, resulting in the disruption of photosynthesis as well as a threat to the aquatic animals and plants [5,6]. Besides, it provides the conditions for anaerobic treatment that disturb the entire ecological cycle including the self-treatment system [7]. So, removal of dyes from effluents before discharging them to the environment is necessary.

Various technologies such as chemical oxidation, ultrafiltration [8], coagulation and flocculation [9], activated carbon [10], and adsorption [11] have been applied for dye removal from textile effluents. Among these methods, flocculation and sorption are the most suitable methods for removing disperse dyes and other suspended particles [12]. Recently, iron-polyphenol complexes have been introduced as adsorptive flocculants for dye removal from wastewaters [13]. Metal-polyphenol complexes have been synthesized using aqueous extract of all plant parts including flowers, fruits, leaves, bark, and roots [14]. Plant phenolic compounds show a high tendency to chelate with metals and form metal complexes [15]. Wang *et al.* synthesized the iron-polyphenol complex nanoparticles using Sage leaves and stated that hydroxyl groups on phenolic acids, terpenoids, and flavonoids in the plant play a key role in the iron-complexes formation [16]. They also tested the removal of cationic dye ethyl violet with synthesized cross-linked Fe-Sage nanomaterial colloids to confirm that its surface charge is positive. In another study, they found that polyphenols gradually cross-linked after a few days and formed polymeric condensed iron-polyphenol complexes [17]. Aoudia *et al.* reported that phenolic acids such as *p*-coumaric, ferulic, and caffeic acids, as well as the flavonols of rutin, and isoquercetin are the main compounds of Melia azedarach water extract [18].

In the present study, it is attempted to synthesize iron-polyphenol nanohydrogel (Fe-PNG) from aqueous fruits extract of Melia azedarach as a chelating and reducing agent [19]. The structure of synthesized Fe-PNG is studied by Fourier transform infrared spectroscopy (FTIR), field emission scanning electron microscopy (FESEM), X-ray diffraction (XRD), Brunauer-Emmett-Teller (BET) analysis, and zeta potential. Furthermore, its ability for flocculation and the removal of Disperse Yellow 211 dye from aqueous solutions is investigated.

EXPERIMENTAL

Reagents and Instruments

Iron(III) chloride hexahydrate (99%) was purchased from Sigma-Aldrich (St. Louis, MO, USA). Disperse Yellow 211 (DY211) was obtained from Kimia Kavir Co. (Yazd, Iran). Melia azedarach fruits were collected from the Greenspace of Yazd university campus. A stock solution of 350 mg l^{-1} of DY211 was prepared by dissolving 350.0 mg of the reagent in 1000 ml distilled water. The working solutions were prepared by proper dilution of stock solution with water.

The FT-IR spectra were recorded with KBr pellet using a Bruker spectrophotometer (Bruker Optics, Karlsruhe, Germany). The morphology of the hydrogel was investigated by the field emission scanning electron microscopy instrument (Zeiss Sigma FESEM, Germany). X-ray powder diffraction (XRD) patterns of the synthesized Fe-PNG were achieved using PANalyticalX'Pert Pro diffractometer (Almelo, The Netherlands) and the zeta potential value of swollen flocculants was determined by HORIBA SZ-100. The BET analysis of synthesized Fe-PNG was measured by mercury porosimeter (Thermo Scientific, Pascal 140, USA). A single-beam UV-Vis spectrophotometer (Jenway 6300, Essex, UK) with 1.0 cm glass cells was used to measure the absorbance.

Preparation of the Fe-PNG

Iron-polyphenol nanohydrogel (Fe-PNG) was synthesized via the green method using Melia azedarach fruits. Briefly, Melia azedarach fruits extract was prepared by adding 5.0 g of Melia azedarach fruits powder to 100 ml hot water (~ 90 ºC) under magnetic stirring. The mixing was continued until it was cool to room temperature and filtered. In the next step, Melia azedarach fruit extract along with a separately prepared solution of 0.05 M of $FeCl_3.6H_2O$ was bubbled with nitrogen gas for 20 min and an equal volume of these solutions was mixed under a nitrogen atmosphere for 5 min. Finally, the mixture was dried in a vacuum oven at 50 °C and stored for subsequent study. The chemical structure of the Fe-PNG is shown in Fig. 2.

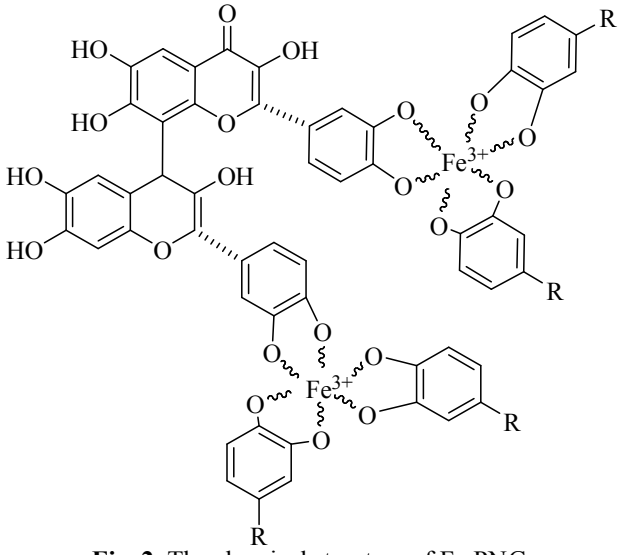

Fig. 2. The chemical structure of Fe-PNG.

Sorption Studies

The sorption study was done with the batch method. Thus, the pH of the dye solution was adjusted to ~ 6 using hydrochloric acid (0.1 M) or sodium hydroxide (0.1 M). Batch mode sorption experiments were carried out by adding 9 mg of the prepared Fe-PNG into 30 ml of DY211 dye solution (150-350 mg l^{-1}) with pH 6.0 at room temperature. The mixture was stirred by a mechanical stirrer at 250 rpm for 20 s and was left for 1 h for the achievement of equilibrium and settle down of the sorbent. Then, the mixture was filtered and the amount of dye in the solution was measured at 487 nm (λ_{max} of dye) by the UV-Vis spectrophotometer. The amounts of dye sorbed on the sorbent at the equilibrium (q_e (mg g^{-1})) and the removal efficiency (R%) of the sorbent were computed using the following equations:

$$q_e = \frac{(C_0 - C_e)V}{W} \quad (1)$$

$$R\% = \frac{(C_0 - C_e)}{C_0} \times 100 \quad (2)$$

where C_0 and Ce (mg l^{-1}) are the initial and equilibrium concentrations of DY211 in the aqueous phase, respectively, V (l) is the volume of dye solution and W (g) is the weight of sorbent.

Sorption Kinetics, Thermodynamics, and Isotherms Calculations

The sorption kinetics of disperse dye on the Fe-PNG *versus* time was studied with a dye solution at pH 6.0 and an initial concentration of 250 mg l^{-1}. The mixture was stirred by a mechanical stirrer for 20 s at room temperature and then sampling was carried out at various time intervals. The amount of DY211 sorbed on the Fe-PNG at time t (q_t, mg g^{-1}) was determined using the following equation:

$$q_t = \frac{(C_0 - C_t)V}{W} \quad (3)$$

where q_t is the amount of DY211 sorbed at time t (mg g^{-1}), C_0 and C_t are initial, and at time t concentration of dye, respectively, V is the solution volume (l), and W is the amount of sorbent (g).

The sorption process kinetics of the DY211 on the Fe-PNG was analyzed based on the pseudo-first-order [20], pseudo-second-order [21], and Elovich [22] models. The linear form of these models is expressed by the equations of (4) to (6), respectively.

$$\ln(q_e - q_t) = \ln q_e - K_1 t \quad (4)$$

$$\frac{t}{q_t} = \frac{1}{K_2 q_e^2} + \frac{t}{q_e} \quad (5)$$

$$q_t = \frac{1}{\beta \ln \alpha\beta + \frac{1}{\beta}} \ln t \quad (6)$$

In these equations, q_e and q_t are the amounts of dye sorbed (mg g^{-1}) at the equilibrium and at any time t, respectively, and K_1 (min^{-1}) and K_2 (g mg^{-1} min^{-1}) denote the rate constants of pseudo-first-order and pseudo-second-order adsorption, respectively. α and β are the Elovich coefficients, α is the initial adsorption rate constant (mg g^{-1} min^{-1}) and β is related to the extent of the surface coverage and the activation energy for chemisorption (g mg^{-1}) and are calculated from the plot of q_t against ln t. The pseudo-first-order and the pseudo-second-order models mimic the surface-controlled sorption rate, whereas, the Elovich kinetic model revealed that the sorption is limited by the surface-controlled sorption onto energetically

heterogeneous sites [20].

The mechanism of interaction of DY211 molecules with nanohydrogel was investigated by considering the sorption isotherms and comparing the determination coefficients (R^2). The experiments were performed at the optimized pH by the addition of 9 mg of the prepared Fe-PNG to 30 ml of different concentrations of DY211 solutions. The interaction of DY211 molecules and sorbent was evaluated by fitting the experimental results to the Langmuir (7), Temkin (8), and Freundlich (9) isotherm models. The corresponding linearized equations are:

$$\frac{C_e}{q_e} = \frac{1}{q_m K_L} + \frac{1}{q_m} C_e \quad (7)$$

$$q_e = A \ln K_T + A \ln C_e \quad (8)$$

$$\ln q_e = \ln K_f + \frac{1}{n} \ln C_e \quad (9)$$

In these equations, q_m (mg g^{-1}) and K_L (l mg^{-1}), the Langmuir isotherm constants, are corresponding to the maximum monolayer sorption capacity and sorption energy, respectively. C_e (mg l^{-1}) and q_e (mg g^{-1}) are the equilibrium concentration of DY211 in solution and equilibrium sorption capacity, respectively. K_T, Temkin isotherm equilibrium binding constant (mol^{-1}), is indicating the maximum binding energy and A is the sorption heat constant. K_f (mg g^{-1}) and n are the Freundlich constants corresponding to the relative sorption capacity of the sorbent and sorption intensity, respectively.

The Langmuir theory assumes that the sorbent structure is homogeneous, and the sites of sorption have equivalent energy and are indistinguishable. According to this model, the rate of sorption is proportional to the concentration of DY211 in the solution as well as the specific surface area. Temkin model is based on the assumption that the heat of sorption of molecules to the layer linearly diminishes with the surface coverage due to the interaction of sorbent with dye. The Freundlich isotherm assumes heterogeneous sorbent structures with multilayer reversible sorption.

The Gibbs free energies ΔG^o for the DY211 sorption onto Fe-PNG were calculated by performing several experiments at 293, 303, 313, and 323 K temperatures, using the following equation:

$$\Delta G^\circ = -RT \ln K_C \quad (10)$$

$$K_C = \frac{q_e}{C_e}$$

In these equations, K_C is the equilibrium constant, q_e and C_e are the quantity of dye per unit mass of sorbent and the equilibrium concentration of the analyte in solution, respectively, T is the temperature in Kelvin and R is the ideal gas constant. The change in enthalpy in sorption (ΔH^o) and the entropy change in sorption (ΔS^o) were determined using the equation of Van't Hoff:

$$\ln K_C = \frac{\Delta S^\circ}{R} - \frac{\Delta H^\circ}{RT} \quad (11)$$

RESULTS AND DISCUSSION

The addition of ferric ions to the prepared Melia azedarach fruits extract resulted in the rapid cross-linking of its polyphenolic compounds and the formation of polymeric condensed iron-polyphenol nanohydrogel [17]. Upon cross-linking, the pH of the extract solution was rapidly decreased from 4.0 to 1.4 due to the replacement and release of the protons of the polyphenols of Melia azedarach fruits with Fe^{3+} and the formation of a polymeric gel [16]. The association of the process of cross-linking of Fe-PNG with the decrease in the pH and precursors' color change indicates the high affinity of the polyphenolic compounds of Melia azedarach fruits extract for metal chelation [23]. This observation confirms the rapid reaction of iron(III) chloride with polyphenols and is consistent with the previous reports of the high metal-chelating ability of Melia azedarach extract [24]. The ability of the designed sorbent to remove the dye is demonstrated by showing the UV spectra of the DY211 before and after sorption by the Fe-PNG (Fig. 3).

Characterization of Melia Azedarach Fruits Dried Extract and Fe-PNG

The FT-IR spectra of the dried Melia azedarach fruits extract and Fe-polyphenol complex are provided in Fig. 4. The band observed at 3400 cm^{-1} corresponds to O–H of H

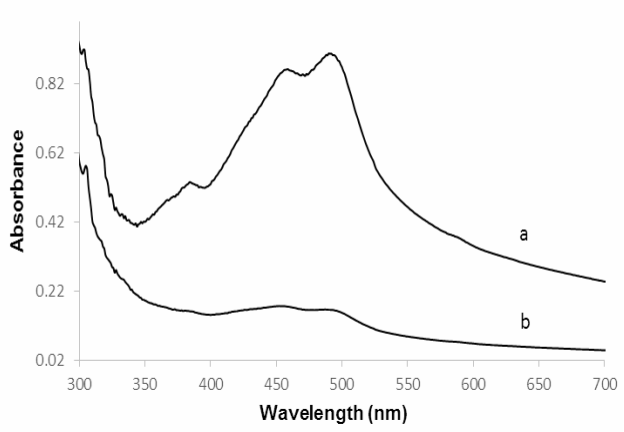

Fig. 3. UV spectra of DY211 (200 mg l^{-1}) before (a) and after (b) sorption process by 7 mg Fe-PNG from 30 ml of solution.

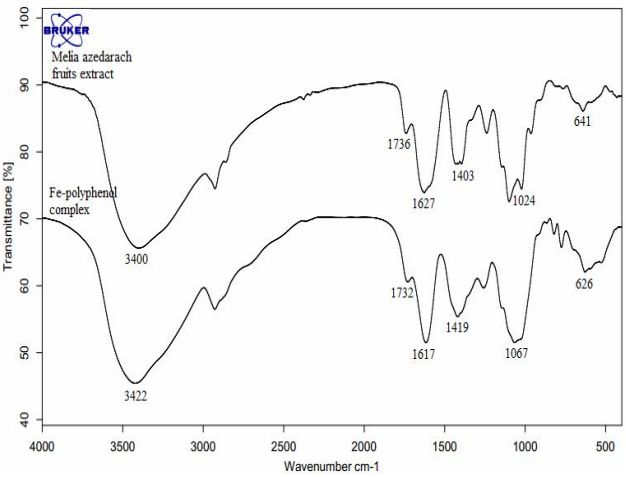

Fig. 4. Infrared spectra of Melia azedarach and Fe-polyphenol complex nanohydrogel.

bond or carboxylic acids [17]. The absorption bands at 1627 and 1403 cm^{-1} are assigned to carboxylate characteristically [25]. The band at 1736 cm^{-1} of Melia azedarach fruits is related to the C=O of carboxylic acid, while the band around 1024 cm^{-1} could be attributed to the C–O of carboxylic acid [17]. The characteristic bands of dried Melia azedarach fruits extract with some shifts (at 3422, 1732, 1617, 1419, and 1067 cm^{-1}) are also observed in Fe–Melia azedarach polyphenol complex spectrum. The O–H functional group

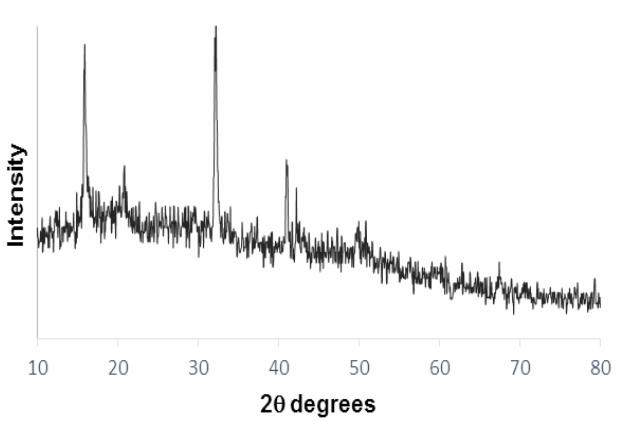

Fig. 5. XRD pattern of Fe-PNG.

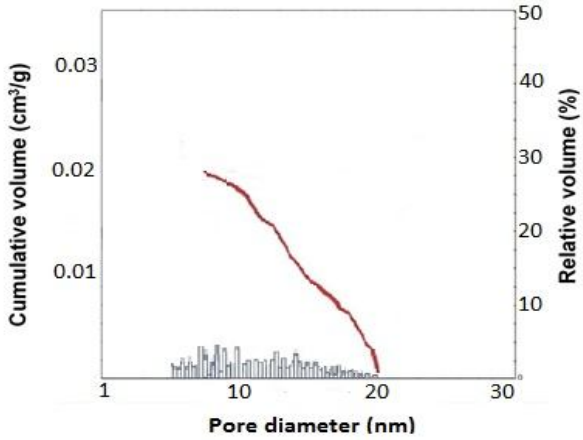

Fig. 6. BET analysis of Fe-PNG.

on Fe-PNG helps the formation of hydrogen bonds with dye functional groups, leading to dye coagulation [16].

The XRD pattern of synthesized Fe-PNG (Fig. 5) represents the peaks at 2θ of 15.9 and 20.8° corresponding to the polyphenol and iron hydroxide, respectively, and the peaks appeared at 2θ of 32.2, and 37.3° is characteristic of the mineral complex [26].

BET analysis of freeze-dried synthesized Fe-PNG was carried out and its results are shown in Fig. 6. Specific surface area, cumulative volume, and the pore size range for Fe-PNG were 4.13 m^2 g^{-1}, 0.0228 cm^3 g^{-1}, and 5.2-19.7 nm, respectively.

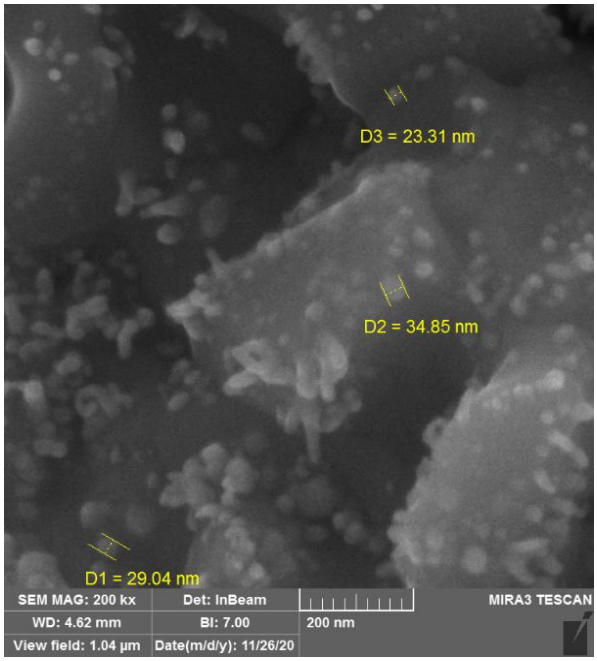

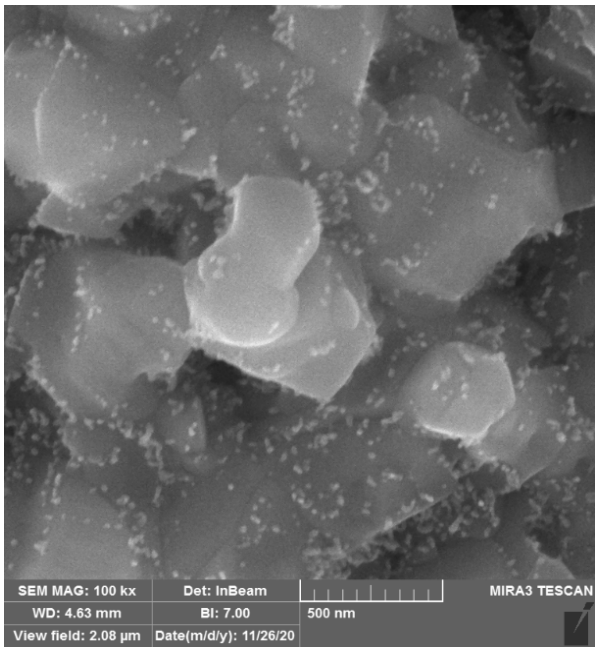

Fig. 7. FESEM images of Fe-PNG (a) Low-magnification, (b) High-magnification.

The FESEM image of cross-linked Fe-PNG (Fig. 7) indicated the presence of Fe-melia azedarach nanoparticles with the size in the range of 23-35 nm and the formation of

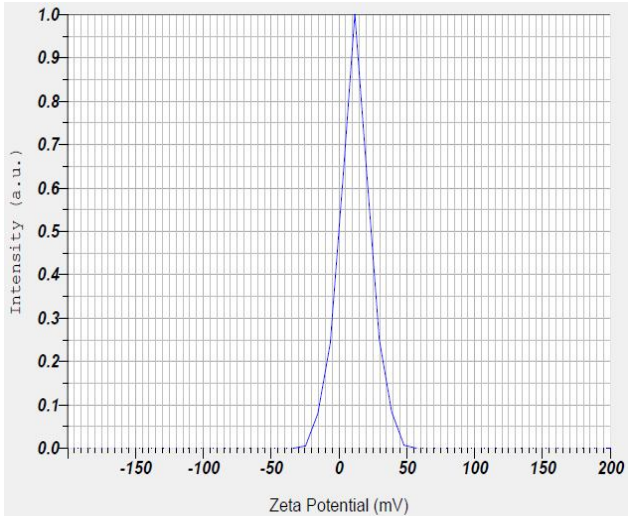

Fig. 8. Zeta potential of Fe-PNG.

an extended network of Fe-polyphenols. The zeta potential of sorbent was found to be +11.8 mV (Fig. 8). The positive charge of Fe-PNG helps the increase in the sorption capacity as well as the kinetics of sorption of DY211 [4].

Effects of Contact Time and Initial DY211 Concentration

The time needed to attain equilibrium and the kinetics of the sorption of DY211 on Fe-PNG were studied by conducting some experiments with the addition of 9 mg of the prepared Fe-PNG gel into 30 ml of various initial dye concentrations (150, 200, and 250 mg l^{-1}), at room temperature and pH 6.0. The results (Fig. 9) revealed that the uptake of DY211 is rapid in the first 10 min, and then slows down until it reaches the saturation state at about 40 min. This observation can be related to the higher driving force of the transfer of DY211 molecules toward the active site of the sorbent. Thus, in the early stage, where the amount of dye and the unoccupied active sites are higher, the speed of uptake is faster. Furthermore, Fig. 9 revealed that an increase in the initial concentration of dye from 150 to 250 mg l^{-1} resulted in an increase in the amount of DY211 sorption to the Fe-PNG from 464.86 mg g^{-1} to 791.01 mg g^{-1}. By increasing the dye concentration, the number of collisions of DY211 molecules with the sorbent surface increases, resulting in the growth of heavier

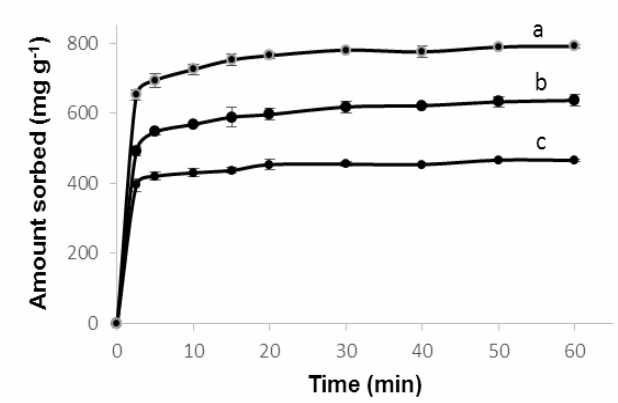

Fig. 9. The effect of contact time and initial concentrations (150 (a), 200 (b), and 250 mg l^{-1} (c)) on the removal of DY211 by 0.3 g l^{-1} of Fe-PNG in pH 6.0, mixing rate 250 rpm and room temperature.

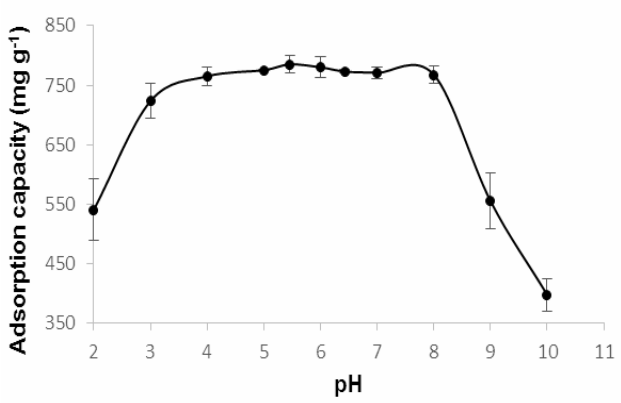

Fig. 11. The effect of pH changes on sorption of DY211 onto sorbent (Fe-PNG). Conditions: contact time 60 min, dye concentration 200 mg l^{-1}, mixing rate 250 rpm, 0.23 g l^{-1} of sorbent, and room temperature.

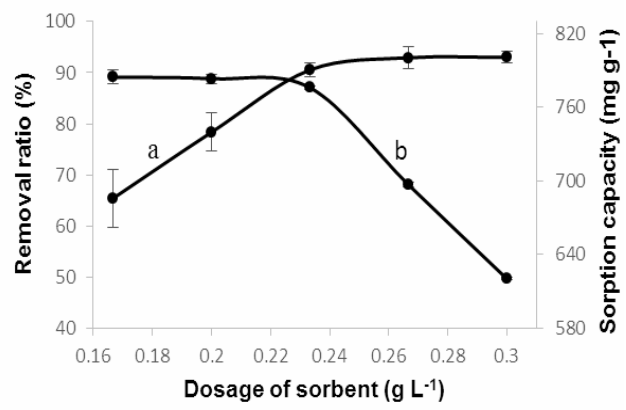

Fig. 10. (a) The effect of sorbent dosage on removal ratio of DY211, and (b) sorption capacity at room temperature. Conditions: Dye concentration 200 mg l^{-1}, pH 6.0, and the equilibration time (60 min).

flocculate and consequently faster sedimentation.

Effect of Flocculant Dosage

The effects of different amounts of Fe-PNG (0.16-0.3 g l^{-1}) on the removal of DY211 from 30 ml solution with the initial concentration of 200 mg l^{-1} was studied under the conditions of room temperature, pH of 6.0, equilibration time of 1 h and stirring rate of 250 rpm. As shown in Fig. 10a, the removal ratio of DY211 is increased with increasing flocculant dosage up to ~ 0.23 g l^{-1} and levels off at its higher amount. Thus, 0.23 g l^{-1} of Fe-PNG, is capable of removal of more than 90% of dye. Figure 10b indicates that the sorption capacity decreased with increasing sorbent dosage. This phenomenon can be due to the amount of available vacant sorption sites of Fe-PNG. At the low dosage of flocculant, the active sites are completely occupied, resulting in higher calculated sorption capacity. However, with the higher amounts of Fe-PNG, the system readily approaches equilibrium while all the available active sites are not occupied, resulting in the calculation of lower sorbent capacity at the fixed dye concentration [27]. The maximum sorbent capacity was calculated as 772.5 mg of DY211 per gram of the sorbent.

Influence of pH

The pH of the solution may affect the degree of interaction of DY211with sorbent and its removal. The effect of the pH in the range of 2.0-10.0 on the sorption of DY211 (200 mg l^{-1}) from 30 ml solution onto the 7.0 mg of Fe-PNG under other optimized conditions was investigated (Fig. 11). The sorption capacity of Fe-PNG is maximum in the pH range of 4.0-8.0. In low pHs, the dye becomes

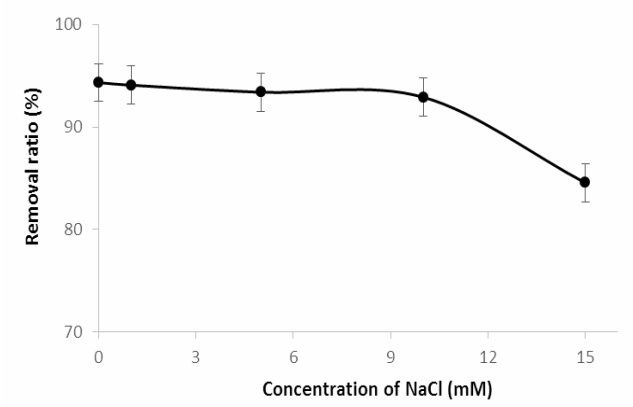

Fig. 12. Effect of ionic strength on dye removal. Conditions: pH 6.0, contact time 60 min, dye concentration 250 mg l^{-1}, mixing rate 250 rpm, 0.23 g l^{-1} of sorbent, and room temperature.

positively charged due to the protonation resulting in its repulsion with the positively charged sorbent. The decrease in pH higher than 8.0 can be related to the deprotonation of phenolic groups of the sorbent followed by its decrease in hydrogen bonding with the dye.

Effect of Ionic Strength

The effect of ionic strength on the removal of DY211by Fe-PNG was investigated by performing a series of experiments with a constant concentration of dye and varying amounts of NaCl (5.0-15.0 mM). The results demonstrated (Fig. 12) that up to 10.0 10.0 mM of salt, the removal of dye by the Fe-PNG is maximum and constant, but a further increase in the concentration of salt causes a decrease in dye sorption. This can be due to the involvement of some of the hydroxyl groups with sodium resulting in the reduction of hydrogen-bonding with dye molecules. Thus, at a high concentration of NaCl, the hydrogel sorbent is less swollen (followed by a decrease in flocculant properties), the mass transfer in the aqueous solution is reduced and subsequently, the dye removal is decreased.

Sorption Isotherms, Kinetics, and Thermodynamics Study

To investigate the binding and equilibrium behavior of the prepared Fe-PNG with DY211 molecules, the

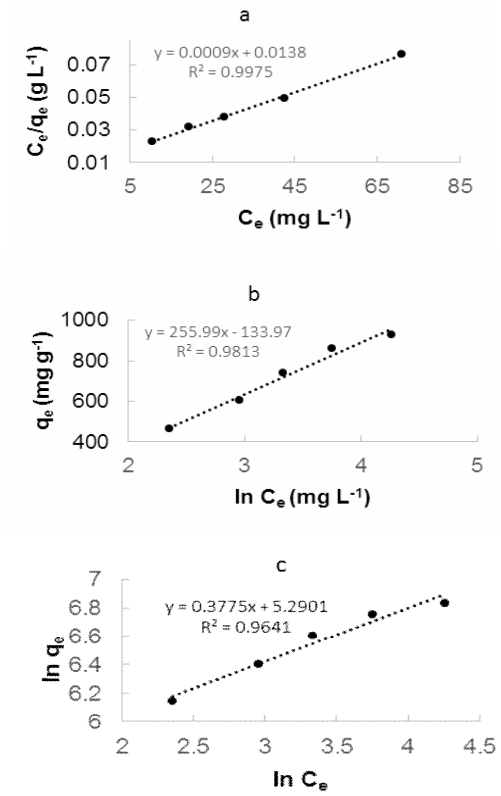

Fig. 13. (a) Langmuir, (b) Temkin, and (c) Freundlich isotherms for sorption of DY211 by Fe-PNG sorbent (mixing rate = 250 rpm, sorbent dosage = 0.3 g l^{-1}, temperature = 25 °C, pH 6.0).

experimental data were fitted to various isotherms including Langmuir, Temkin, and Freundlich. The linear graphs of these isotherm models (Fig. 13) and the related fitted constants (Table 1) revealed that the Langmuir plot (Fig. 13a) with the R^2 value of 0.9975 is best fitted to the experimental data. Thus, the sorption process of DY211 on the Fe-PNG surfaces is a monolayer with homogeneous surface sorption. The value of q_{max} (maximum capacity of sorbent) was found to be 1111.1 mg g^{-1} indicating the high ability of the green-based sorbent for DY211 removal.

To study the sorption kinetics of DY211 on Fe-PNG, the experimental data were fitted to the pseudo-first-order, pseudo-second-order, and Elovich kinetic models. The linear fitting curves of the kinetic models (Fig. 14) and k, q_e, α, β and determination coefficient (R^2) (Table 1) show that R^2 for the pseudo-second-order (0.9987) is nearer to unity

Table 1. Isotherm and Kinetic Parameters for YD211 onto Fe-PNG

Isotherm & kinetic models	Parameters	Value
Langmuir	q_m (mg g^{-1})	1111.11
	K_L (l mg^{-1})	0.0652
	R^2	0.9975
Temkin	A	255.99
	K_T (mol^{-1})	0.5925
	R^2	0.9813
Freundlich	K_f (mg g^{-1})	198.36
	n	2.6490
	R^2	0.9641
pseudo-first order	q_e (mg g^{-1})	318.01
	K_1 (min^{-1})	0.0473
	R^2	0.9460
pseudo-second order	q_e (mg g^{-1})	1000.00
	K_2 (g mg^{-1} min^{-1})	0.0004
	R^2	0.9987
Elovich	α	83872.1
	β	0.0108
	R^2	0.9169

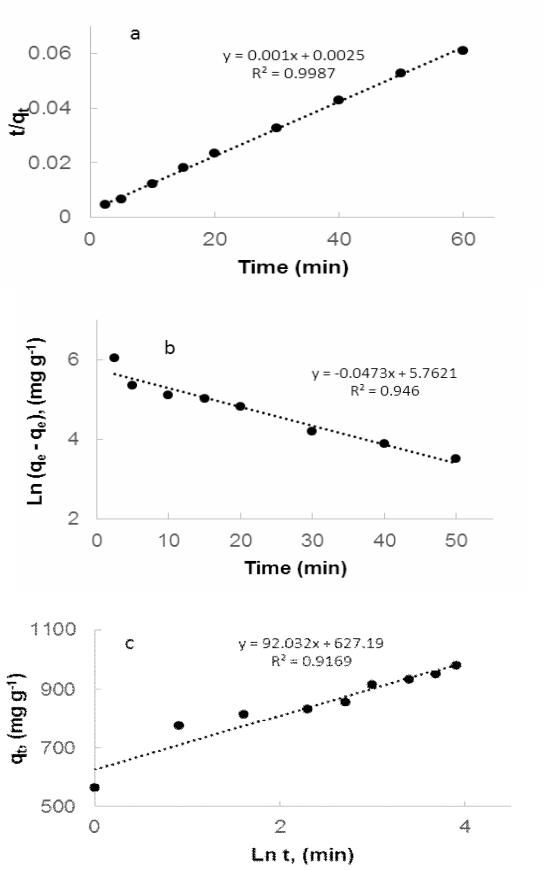

Fig. 14. (a) The linear plot of the pseudo-second-order, (b) pseudo-first-order, (c) Elovich models for sorption kinetics of DY211 by Fe-PNG sorbent (mixing rate = 250 rpm, initial dye concentration = 250 mg l^{-1}, sorbent dosage = 0.3 g l^{-1}, pH 6.0 and 25 °C).

(Fig. 14a) than pseudo-first-order (0.9460) (Fig. 14b) and Elovich (0.9169) (Fig. 14c) models, indicating the suitability of the pseudo-second-order. Thus, the rate-controlling step in the DY211 sorption process is chemical sorption.

The thermodynamic parameters were calculated by fitting the data to the Van't Hoff equation and the result are shown in Table 2. The amounts of $\Delta G°$ are negative at all temperatures indicating the spontaneous sorption process. The negative value of $\Delta H°$ indicated that the sorption process is exothermic. The positive amount of $\Delta S°$ for the sorption of the disperse dye on Fe-PNG denotes an increase in the randomness of the sorption as well as the affinity of the Fe-PNG for the DY211 [28].

Application of the Sorbent to Real Sample

Applicability of Fe-PNG sorbent for the removal of DY211 dye in the remediation of well water and wastewater of Yazdbaf Textile Mills (Yazd, Iran) at the pH of 6.0 was investigated. The results of this study (Table 3) indicate the capability of the Fe-PNG sorbent for the efficient removal of DY211 dye from the investigated sample types.

CONCLUSIONS

In this study, it was demonstrated that the phenolic compounds of Melia azedarach fruits such as phenolic acids rapidly chelate with ferric ions and produce a cross-linked polymeric gel [17,29]. The synthesized gel acted as a flocculant in coagulation and removal of the dispersed yellow 211 dye through hydrogen bonding. The kinetic studies showed that equilibrium sorption of the DY211 occurred at about 50 min by chemical sorption. The sorption

Table 2. Thermodynamic Parameters (ΔG°, ΔH°, and ΔS°) Related to Absorption of DY211 on Fe-PNG at Different Temperatures with 200 mg l^{-1} Concentration and 0.23 g l^{-1} of Sorbent

T (K)	C_e (mg l^{-1})	q_e (mg g^{-1})	K_c	*ΔG°* (kJ mol^{-1})	*ΔH°* (kJ mol^{-1})	*ΔS°* (J mol^{-1} K^{-1})
298	19.43	773.852	39.81	-9.95	-5.87	14.03
303	15.98	788.648	49.34	-10.15		
313	13.62	798.775	58.65	-10.29		
323	11.76	806.734	68.58	-10.37		

Table 3. Removal of DY211 from Real Samples. (Conditions: Sample Volume, 30 ml; Amount of Sorbent = 7 mg; Contact Time, 50 min and pH = 6.0)

Samples	C_0 (mg l^{-1})	C_f (mg l^{-1})	Removal (%)
Waste water[a]	97.0	9.4	90.3
Well Water[b]	200.0	15.9	92.0

[a]Yazdbaf Textile Mills (Yazd, Iran). [b]Yazd University (Yazd, Iran).

Table 4. Comparison of Maximum adsorption Capacity and Equilibrium Time of the Prepared Sorbent with Previously Reported Sorbent for DY211

Composite sorbent	q_m (mg g^{-1})	Equilibrium time	Ref.
Activated carbon	283.30	-	[30]
Gliricidia sepium (WG)	0.253	-	[31]
Isolated Gliriciia sepium cellulose (WGC)	0.499	-	[31]
Cherry stones	105.71	-	[32]
Apricot stones	156.25	-	[32]
Fe-PNG	1111.1	50 min	This work

is exothermic and spontaneous and its mechanism follows the Langmuir isotherm model confirming the monolayer sorption of DY211 to the Fe-PNG. Thus, the iron-polyphenol complex nanohydrogel is suitable for DY211 dye removal. The performance of Fe-PNG towards DY211 dye sorption from aqueous solutions in comparison with other sorbents (Table 4) revealed that Fe-PNG sorbent has a higher sorption capacity (1111.1 mg g^{-1}). Inexpensive and available raw materials, simplicity of sorbent synthesis, biodegradability, rapidity, and high sorption capacity are the main features of the prepared Fe-PNG.

REFERENCES

[1] G. Crini, E. Lichtfouse, Environ. Chem. Lett. 17 (2019) 145.

[2] F. Wei, M.J. Shahid, G.S. Alnusairi, M. Afzal, A. Khan, M.A El-Esawi, Z. Abbas, K. Wei, I.E. Zaheer, M. Rizwan, Sustainability 12 (2020) 5801.

[3] S.M. Abegunde, K.S. Idowu, A.O. Sulaimon, J. Chem. Rev. 2 (2020) 103.

[4] S. Adeel, S.G. Khan, S. Shahid, M. Saeed, S. Kiran, M. Zuber, M. Suleman, N. Akhtar, J. Mex. Chem. 62 (2018) 1.

[5] V. Katheresan, J. Kansedo, S.Y. Lau, J. Environ. Chem. Eng. 6 (2018) 4676.

[6] L.D.O. Yamil, F. Georgin, D.S. Franco, M.S. Netto, E.L. Foletto, D.G. Piccilli, L. Sellaoui, G.L. Dotto, Environ. Sci. Pollut. 28 (2021) 8036.

[7] S. Markandeya, P. Shukla, D. Mohan, Res. J. Environ. Toxicol. 11 (2017) 72.

[8] Y. Long, X. You, Y. Chen, H. Hong, B.-Q. Liao, H. Lin, Sci. Total Environ. 703 (2020) 135540.

[9] N.D.C.L. Beluci, G.A.P. Mateus, C.S. Miyashiro, N.C.

Homem, R.G. Gomes, M.R. Fagundes-Klen, R. Bergamasco, A.M.S. Vieira, Sci. Total Environ. 664 (2019) 222.

[10] M. Ghamsari, T. Madrakian, Anal. Bioanal. Chem. Res. 6 (2019) 157

[11] M.R. Parsaeian, S. Dadfarnia, A.M. Haji Shabani, R. Hafezi Moghaddam, Int. J. Environ. Anal. Chem. (2020). DOI: 10.1080/03067319.2020.1748612.

[12] X. Huang, Y. Wan, B. Shi, J. Shi, H. Chen, H. Liang, Chemosphere 249 (2020) 126129.

[13] L. Szwajkowska-Michałek, A. Przybylska-Balcerek, T. Rogoziński, K. Stuper-Szablewska, Appl. Sci. 10 (2020) 6907.

[14] K.O. Badmus, E. Coetsee-Hugo, H. Swart, L. Petrik, Environ. Sci. Pollut. Res. 25 (2018) 23667.

[15] S. Iravani, B. Zolfaghari, Biomed Res. Int. 2013 (2013) 5.

[16] Z. Wang, C. Fang, M. Mallavarapu, Environ. Technol. Innov. 4 (2015) 92.

[17] Z. Wang, C. Yu, C. Fang, M. Megharaj, Removal of Acid Red 94 and Methylene Blue Using Iron-Polyphenol Nanomaterials Synthesized by Various Plant Leaves: A Comparison Study. International Conference on Nanoscience and Nanotechnology, 2014.

[18] H. Aoudia, N. Ntalli, N. Aissani, R. Yahiaoui-Zaidi, P. Caboni, J. Agric. Food Chem. 60 (2012) 11675.

[19] A. Truskewycz, R. Shukla, A.S. Ball, ACS Omega. 3 (2018) 10781.

[20] Y. Li, H. Xiao, Y. Pan, L. Wang, ACS Sustainable Chem. Eng. 6 (2018) 6994.

[21] R.H. Moghaddam, A.M. Haji Shabani, S. Dadfarnia, J. Environ. Chem. Eng. 7 (2019) 102919.

[22] J.A. Pellicer, M.I. Rodríguez-López, M.I. Fortea, C. Lucas-Abellán, M.T. Mercader-Ros, S. López-Miranda, V.M. Gómez-López, P. Semeraro, P. Cosma, P. Fini, Polymers. 11 (2019) 252.

[23] Y. M'rabet, N. Rokbeni, S. Cluzet, A. Boulila, T. Richard, S. Krisa, L. Marzouki, H. Casabianca, K. Hosni, Ind. Crop. Prod. 107 (2017) 232.

[24] I.E. Orhan, E. Guner, N. Ozturk, F. Senol, S.A. Erdem, M. Kartal, B. Sener, Ind. Crop. Prod. 37 (2012) 213.

[25] R. Lin, A. Li, L. Lu, Y. Cao, Carbohydr Polym. 118 (2015) 126.

[26] A. Ebrahiminezhad, S. Taghizadeh, Y. Ghasemi, A. Berenjian, Sci. Total Environ. 621 (2018) 1527.

[27] X.S. Hu, R. Liang, G. Sun, J. Mater. Chem. A 6 (2018) 17612.

[28] L. Soldatkina M. Zavrichko, Colloids Interfaces 3 (2019) 4.

[29] A.M. El Shafey, Green Process. Synth. 9 (2020) 304.

[30] T. Erdogan, F. Oguz Erdogan, Anal. Lett. 49 (2016) 917.

[31] A.T. Oluwasola, L. Labunmi, O.B. Joseph, A.A. Ojo, A. Olajide, Am. J. Chem. Appl. 5 (2018) 40.

[32] F.O. Erdogan, Tekst. ve Muhendis 24 (2017) 181.